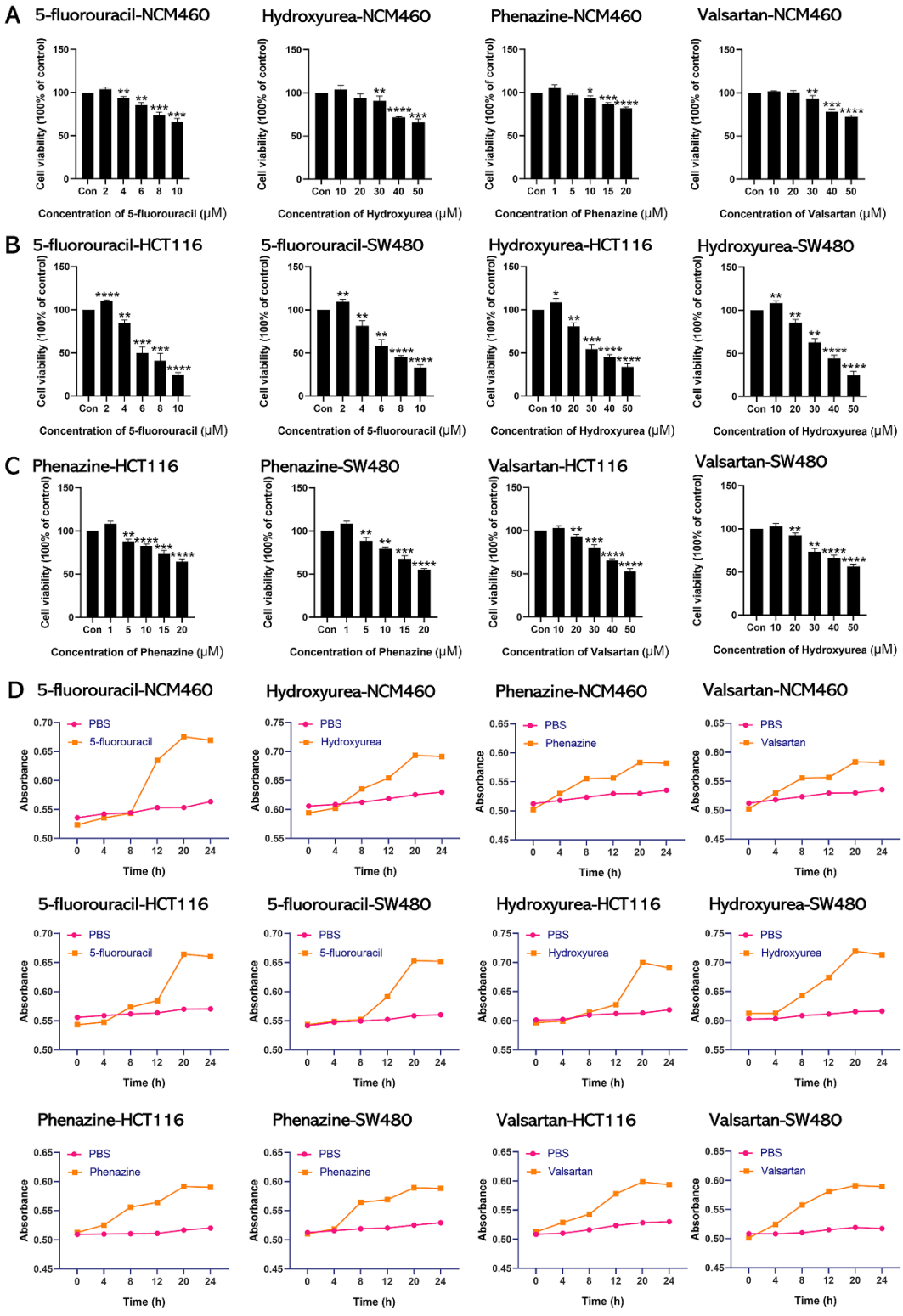

Figure S1 The effect of 5-fluorouracil, hydroxyurea, phenazine and valsartan on proliferation of NCM460, HCT116, and SW480 cells and their uptake efficiency. (A) CCK-8 assay showed the effects of 5-fluorouracil, hydroxyurea, phenazine and valsartan on NCM460 cells. (B)

CCK-8 assay showed the effects of 5-fluorouracil and hydroxyurea on HCT116 and SW480 cells. (C) CCK-8 assay showed the effects of phenazine and valsartan on HCT116 and SW480 cells. (D) The uptake of 5-fluorouracil, hydroxyurea, phenazine and valsartan in NCM460, HCT116 and SW480 cells over time. The data are represented as the mean ± SD (n = 3). Statistical differences were considered significant at * $p < 0.05$, ** $p < 0.01$, *** $p < 0.001$ and **** $p < 0.0001$.

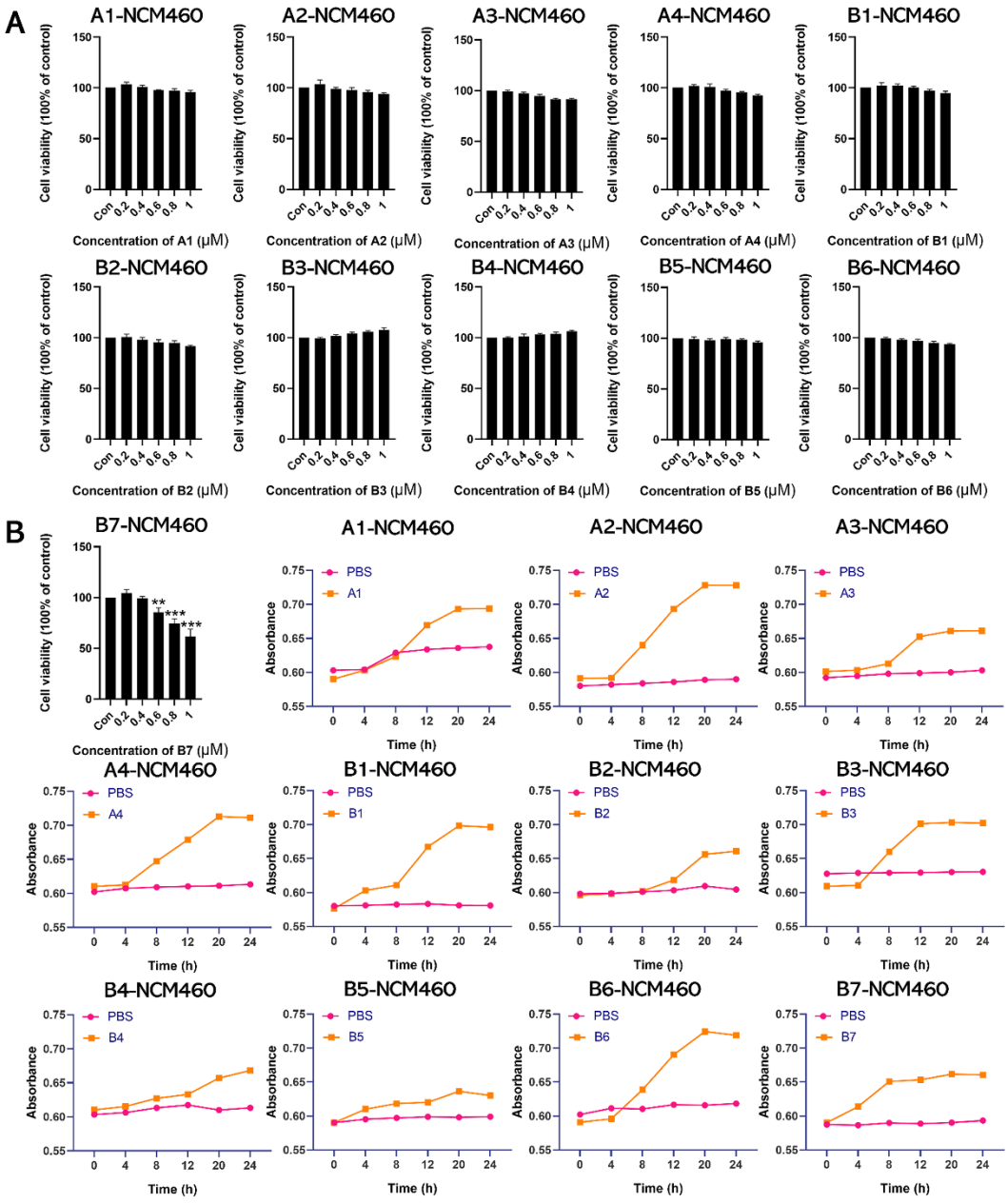

Figure S2 Effects of A1-A4 and B1-B7 on the proliferation of NCM460 cells and their uptake efficiency. (A) CCK-8 assay showed the effects of A1-A4 and B1-B6 on NCM460 cells. (B) CCK-8 assay showed the effect of B7 on NCM460 cells. The uptake of A1-A4 and B1-B7 in NCM460 cells over time. The data are represented as the mean ± SD (n = 3). Statistical differences were considered significant at ** $p < 0.01$ and *** $p < 0.001$.

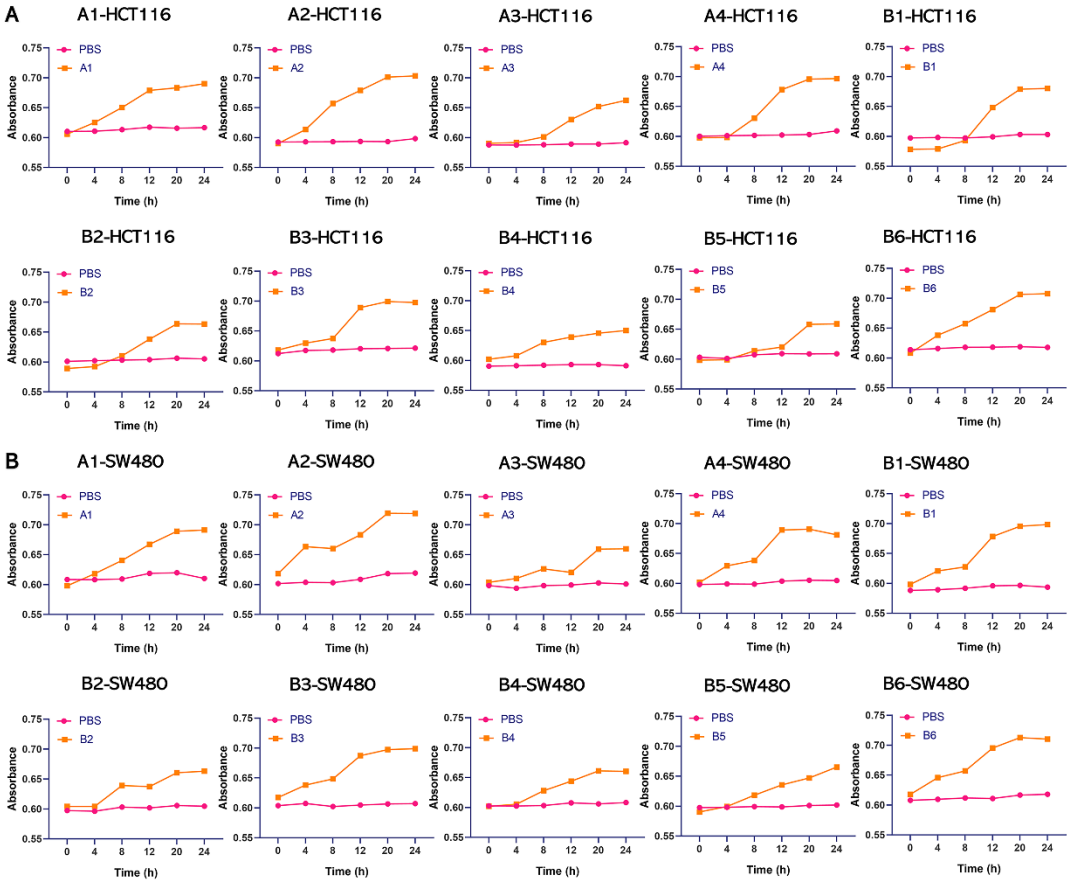

Figure S3 The uptake of A1-A4 and B1-B6 in HCT116 and SW480 cells over time. (A) The uptake of A1-A4 and B1-B6 in HCT116 cells over time. (B) The uptake of A1-A4 and B1-B6 in SW480 cells over time.

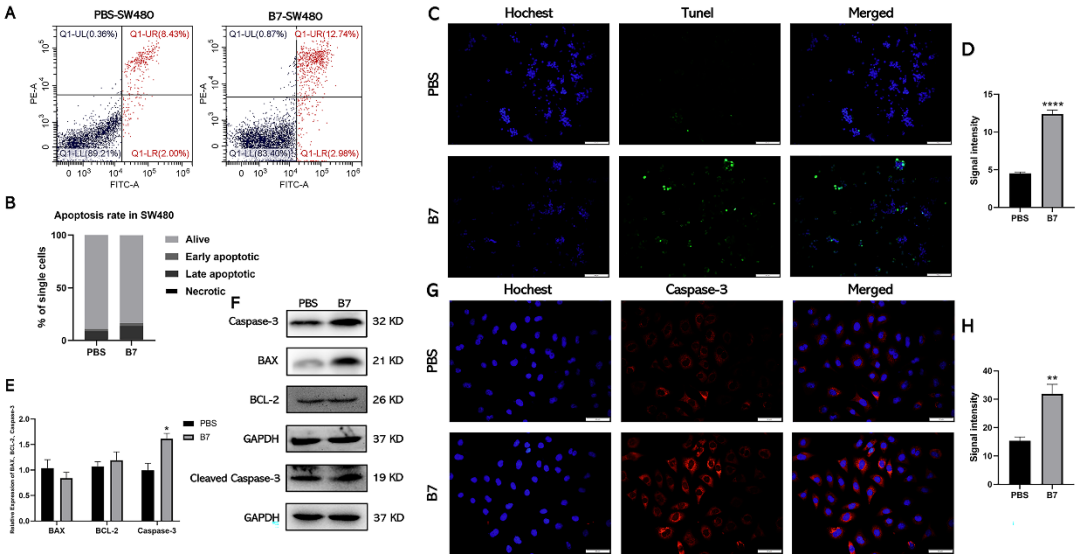

Figure S4 B7 induces apoptosis of CRC cells by promoting the expression of Caspase-3. (A) Flow cytometry was used to analyze the effect of B7 on SW480 cells apoptosis. (B) Statistical analysis of the percentage of SW480 cells undergoing apoptosis. Statistical significances between groups were evaluated using Student t-test for independent groups. (C) TUNEL analysis of SW480 cells treated with B7 (scale bar=100 μm). And associated (D) statistical analysis of TUNEL fluorescence signal intensity. (E) Relative gene expression of apoptosis related genes in SW480 cells treated with PBS or B7. (F) Protein levels of BCL-2, BAX, caspase-3, cleaved Caspase-3 and GAPDH in SW480 cells treated with PBS or B7. (G) Fluorescent signal of Caspase-3 in SW480 cells treated with PBS or B7 (scale bar=50μm). And associated (H) statistical analysis of the Caspase-3 intensity. The data are represented as the mean ± SD (n = 3). Statistical differences were considered significant at * $p < 0.05$, ** $p < 0.01$ and **** $p < 0.0001$.

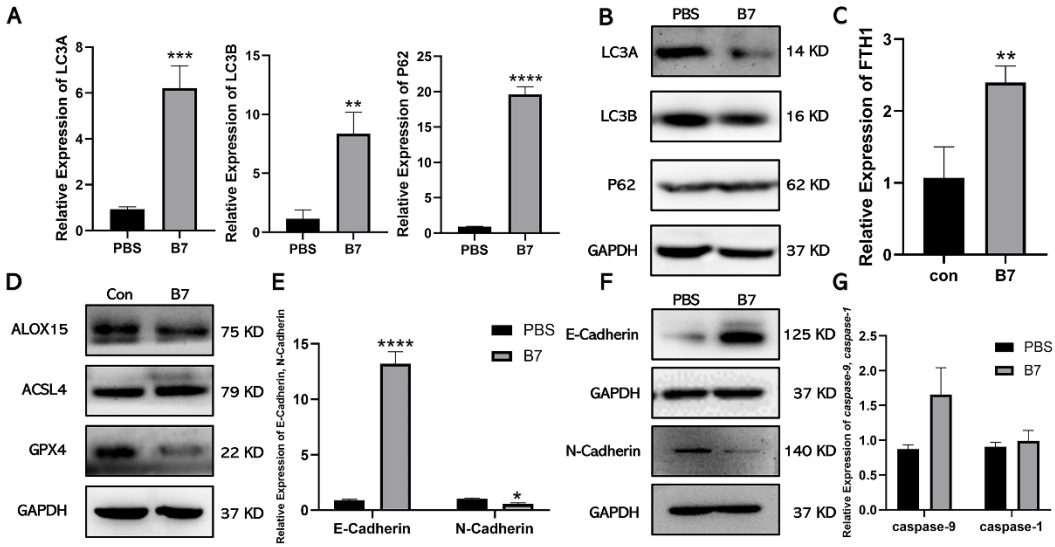

Figure S5 Effect of B7 on the expression of autophagy, feline apoptosis, metastasis and apoptosis-related genes in CRC cells. (A) *LC3A*, *LC3B* and *P62* were analyzed by qPCR. (B) Expression levels of LC3A, LC3B, P62 and GAPDH protein was assessed via Western blotting. (C) *FTH1* were analyzed by qPCR. (D) Expression levels of ALXO15, ACSL4, GPX4 and GAPDH protein was assessed via Western blotting. (E) *E-Cadherin* and *N-Cadherin* were analyzed by qPCR. (F) Expression levels of E-Cadherin, N-Cadherin and GAPDH protein was assessed via Western blotting. (G) *Caspase-9*, *caspase-1* were analyzed by qPCR. The data are represented as the mean ± SD (n = 3). Statistical differences were considered significant at * $p < 0.05$, ** $p < 0.01$, *** $p < 0.001$ and **** $p < 0.0001$.

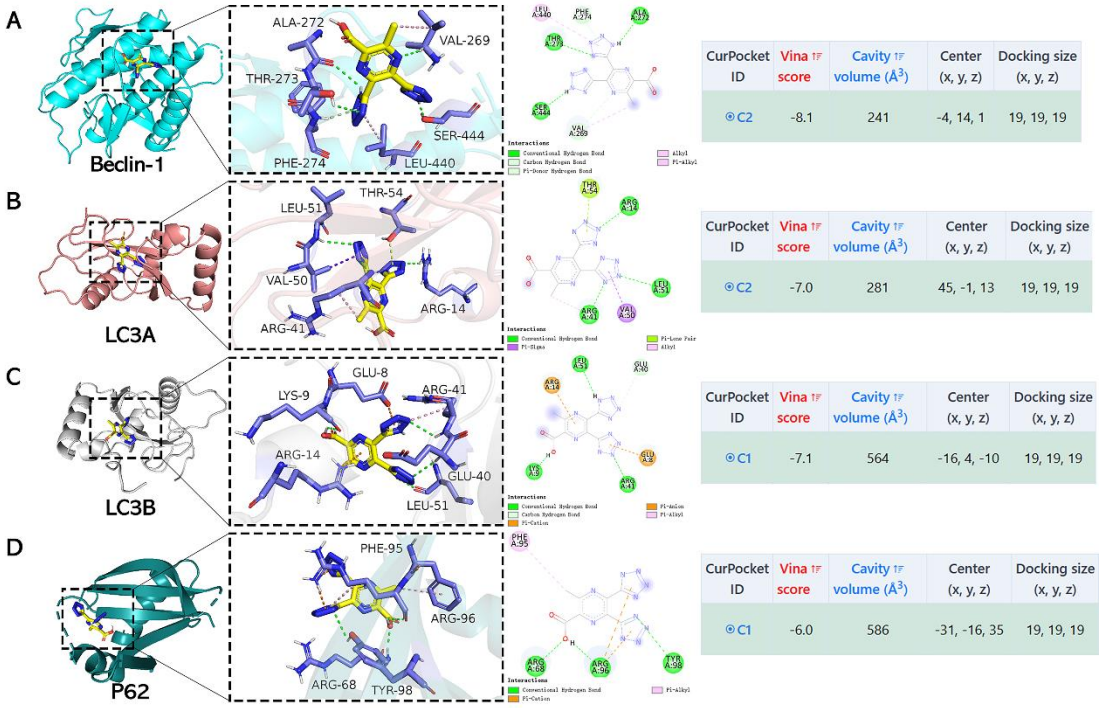

CurPocket ID	Vina score	Cavity volume (Å^3)	Center (x, y, z)	Docking size (x, y, z)
C2	-8.1	241	-4, 14, 1	19, 19, 19

CurPocket ID	Vina score	Cavity volume (Å^3)	Center (x, y, z)	Docking size (x, y, z)
C2	-7.0	281	45, -1, 13	19, 19, 19

CurPocket ID	Vina score	Cavity volume (Å^3)	Center (x, y, z)	Docking size (x, y, z)
C1	-7.1	564	-16, 4, -10	19, 19, 19

CurPocket ID	Vina score	Cavity volume (Å^3)	Center (x, y, z)	Docking size (x, y, z)
C1	-6.0	586	-31, -16, 35	19, 19, 19

Figure S6 Molecular docking of autophagy-associated protein with compound B7. (A) Molecular docking and binding energy analysis of Beclin-1 protein with compound B7. (B) Molecular docking and binding energy analysis of LC3A protein with compound B7. (C) Molecular docking and binding energy analysis of LC3B protein with compound B7. (D) Molecular docking and binding energy analysis of P62 protein with compound B7.

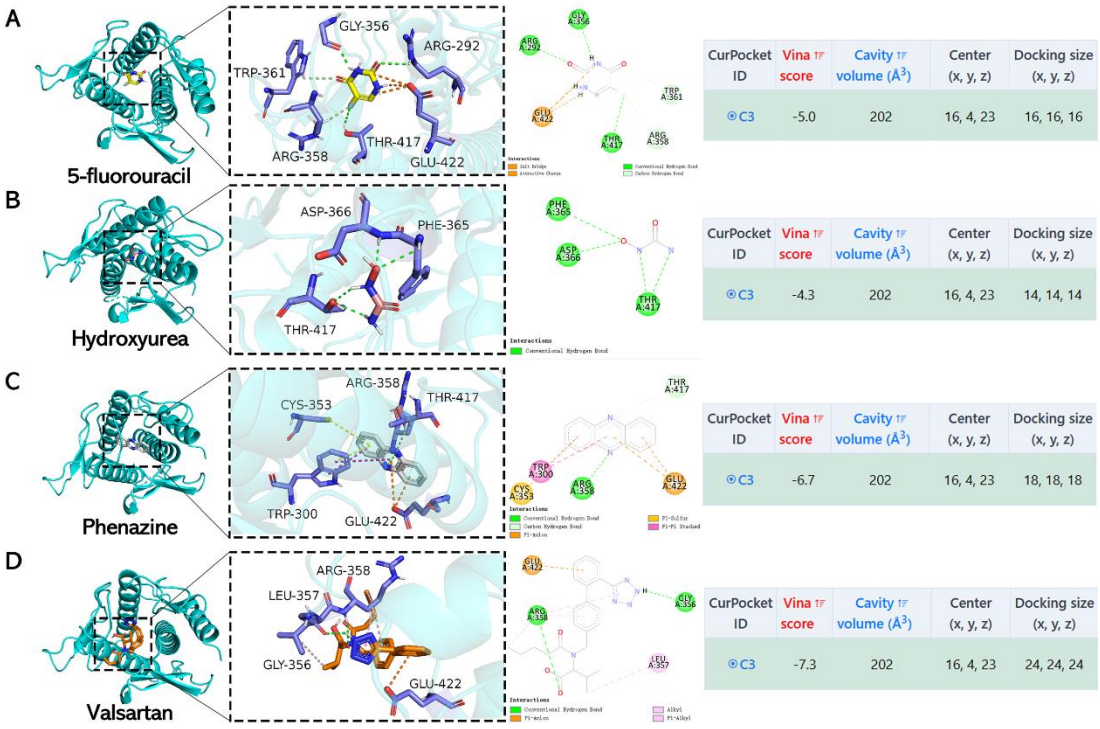

CurPocket ID	Vina score	Cavity volume (Å^3)	Center (x, y, z)	Docking size (x, y, z)
C3	-5.0	202	16, 4, 23	16, 16, 16

CurPocket ID	Vina score	Cavity volume (Å^3)	Center (x, y, z)	Docking size (x, y, z)
C3	-4.3	202	16, 4, 23	14, 14, 14

CurPocket ID	Vina score	Cavity volume (Å^3)	Center (x, y, z)	Docking size (x, y, z)
C3	-6.7	202	16, 4, 23	18, 18, 18

CurPocket ID	Vina score	Cavity volume (Å^3)	Center (x, y, z)	Docking size (x, y, z)
C3	-7.3	202	16, 4, 23	24, 24, 24

Figure S7 Molecular docking of Beclin-1 with compounds 5-fluorouracil, hydroxyurea, phenazine and valsartan. (A) Molecular docking and binding energy analysis of Beclin-1 protein with 5-fluorouracil. (B) Molecular docking and binding energy analysis of Beclin-1 protein with hydroxyurea. (C) Molecular docking and binding energy analysis of Beclin-1 protein with phenazine. (D) Molecular docking and binding energy analysis of Beclin-1 protein with valsartan.

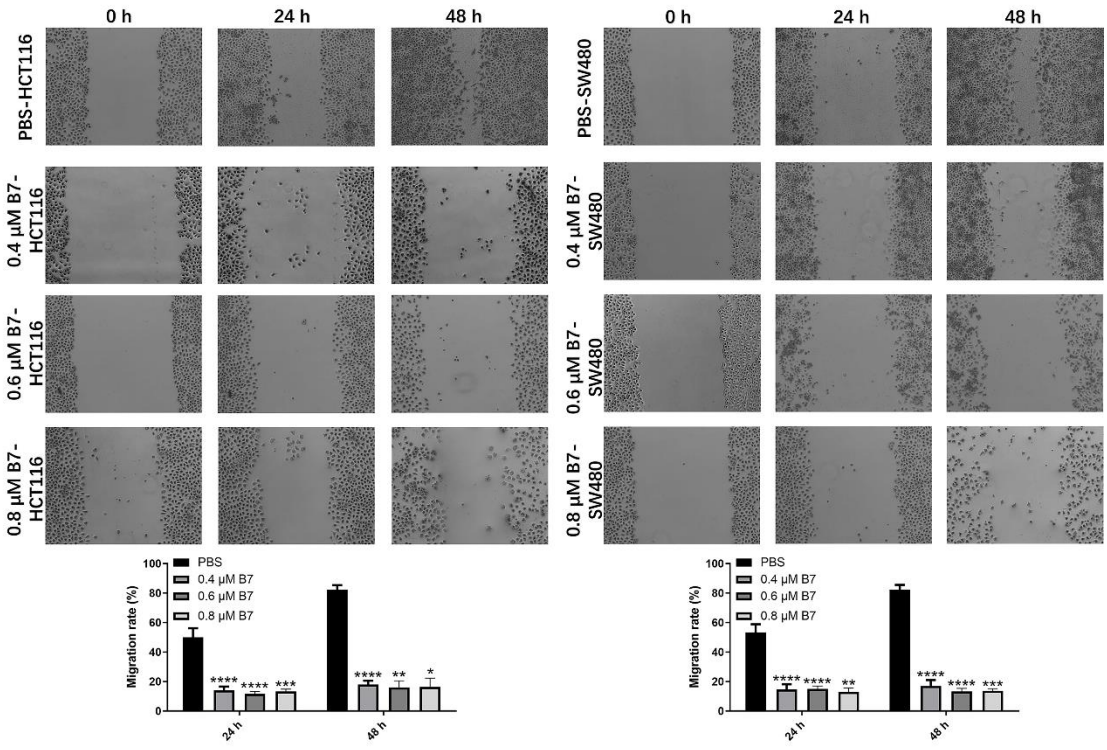

Figure S8 B7 inhibits the migration of CRC. Wound-healing assay images (100× magnification) from HCT116 and SW480 cells treated with PBS and B7 (0.4, 0.6 and 0.8 μM) and statistical analysis of cell migration. Statistical differences were considered significant at * $p < 0.05$, ** $p < 0.01$, *** $p < 0.001$, and **** $p < 0.0001$.

Data S1:

The data of the compound structures examined using ^{1}H NMR, ^{13}C NMR, and HRMS spectra:

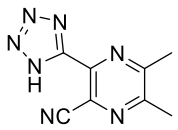

A1

^{1}H NMR (400 MHz, DMSO) δ 2.69 (s, 3H), 2.63 (s, 3H). ^{13}C NMR (101 MHz, DMSO) δ 158.0, 156.4, 153.6, 139.4, 124.0, 116.2, 91.5, 22.7, 22.1.

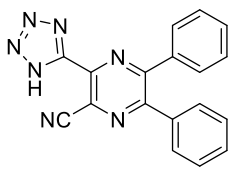

A2

^{1}H NMR (400 MHz, DMSO) δ7.56 – 7.37 (m, 10H). ^{13}C NMR (101 MHz, DMSO) δ 151.2, 150.7, 150.7, 146.9, 139.8, 136.9, 136.3, 133.5, 132.3, 132.3, 127.2, 127.2, 127.1, 115.8.

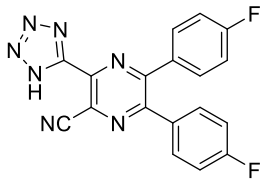

A3

^{1}H NMR (400 MHz, DMSO) δ 7.69 – 7.63 (m, 2H), 7.57 – 7.50 (m, 2H), 7.33 – 7.25 (m, 4H). ^{13}C NMR (101 MHz, DMSO) δ 162.6, 162.3, 154.3, 152.9, 152.7, 139.4, 133.0, 132.8, 132.7, 132.5, 124.2, 116.2.

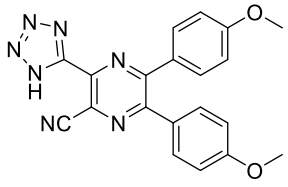

A4

^{1}H NMR (400 MHz, DMSO) δ 3.81 (s, 3H), 3.75 (s, 3H). ^{13}C NMR (101 MHz, DMSO) δ 161.8, 161.3, 153.9, 152.9, 138.6, 132.7, 131.6, 131.1, 129.7, 128.3, 123.6, 116.5, 114.8, 114.5, 55.9, 55.8.

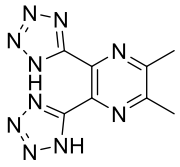

B1

^{1}H NMR (400 MHz, DMSO) δ 2.70 (s, 1H). ^{13}C NMR (151 MHz, DMSO) δ 160.3, 158.3, 141.2, 27.0.

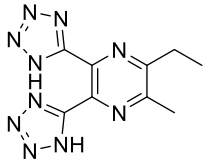

B2

^{1}H NMR (400 MHz, DMSO) δ 3.03 (q, *J* = 7.5 Hz, 1H), 2.73 (s, 1H), 1.32 (t, *J* = 7.3 Hz, 1H). ^{13}C NMR (101 MHz, DMSO) δ 159.1, 155.0, 153.5, 144.8, 143.5, 136.3, 27.6, 21.8, 11.6.

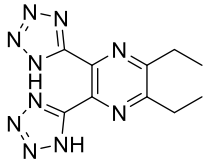

B3

^{1}H NMR (400 MHz, DMSO) δ 3.05 (q, *J* = 7.4 Hz, 1H), 1.33 (t, *J* = 7.4 Hz, 1H). ^{13}C NMR (101 MHz, DMSO) δ 158.6, 153.6, 136.5, 27.1, 12.1.

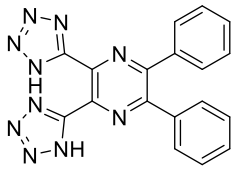

B4

^{1}H NMR (400 MHz, DMSO) δ 7.53 – 7.35 (m, 1H). ^{13}C NMR (101 MHz, DMSO) δ 155.3, 152.8, 137.1, 136.0, 130.3, 130.1, 128.9.

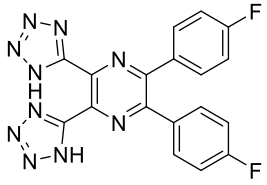

B5

^{1}H NMR (400 MHz, DMSO) δ 7.74 – 7.62 (m, 1H), 7.60 – 7.50 (m, 1H), 7.34 – 7.21 (m, 2H). ^{13}C NMR (101 MHz, DMSO) 164.4 (d, J = 61.5 Hz), 162.8 (d, J = 60.1 Hz), 154.3, 153.7, 151.9, 132.7 (d, J = 8.3 Hz), 116.3 (d, J = 22.0 Hz), 116.0 (d, J = 21.8 Hz).

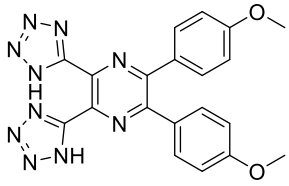

B6

^{1}H NMR (400 MHz, DMSO) δ7.56 –7.52 (m, 4H), 7.31 – 7.22 (m, 4H), 3.78 (s, 6H). ^{13}C NMR (101 MHz, DMSO) δ 158.4, 152.2, 131.1, 129.1, 128.9, 127.5, 113.8, 55.4.

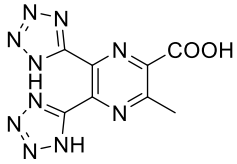

B7

^{1}H NMR (400 MHz, DMSO) δ 2.91 (s, 1H). ^{13}C NMR (101 MHz, DMSO) δ 165.9, 155.5, 153.6, 153.4, 145.0, 140.3, 136.7, 23.1.

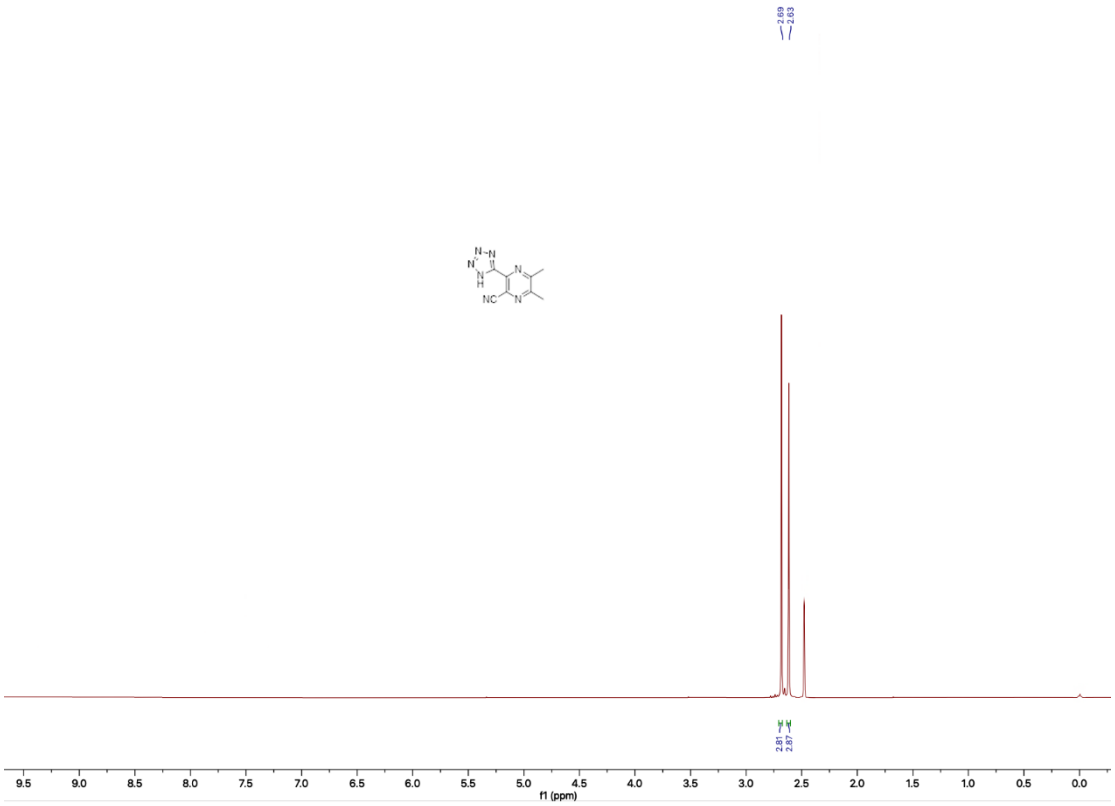
2.69
2.83
2.81
2.87
9.5 9.0 8.5 8.0 7.5 7.0 6.5 6.0 5.5 5.0 4.5 4.0 3.5 3.0 2.5 2.0 1.5 1.0 0.5 0.0
f1 (ppm)

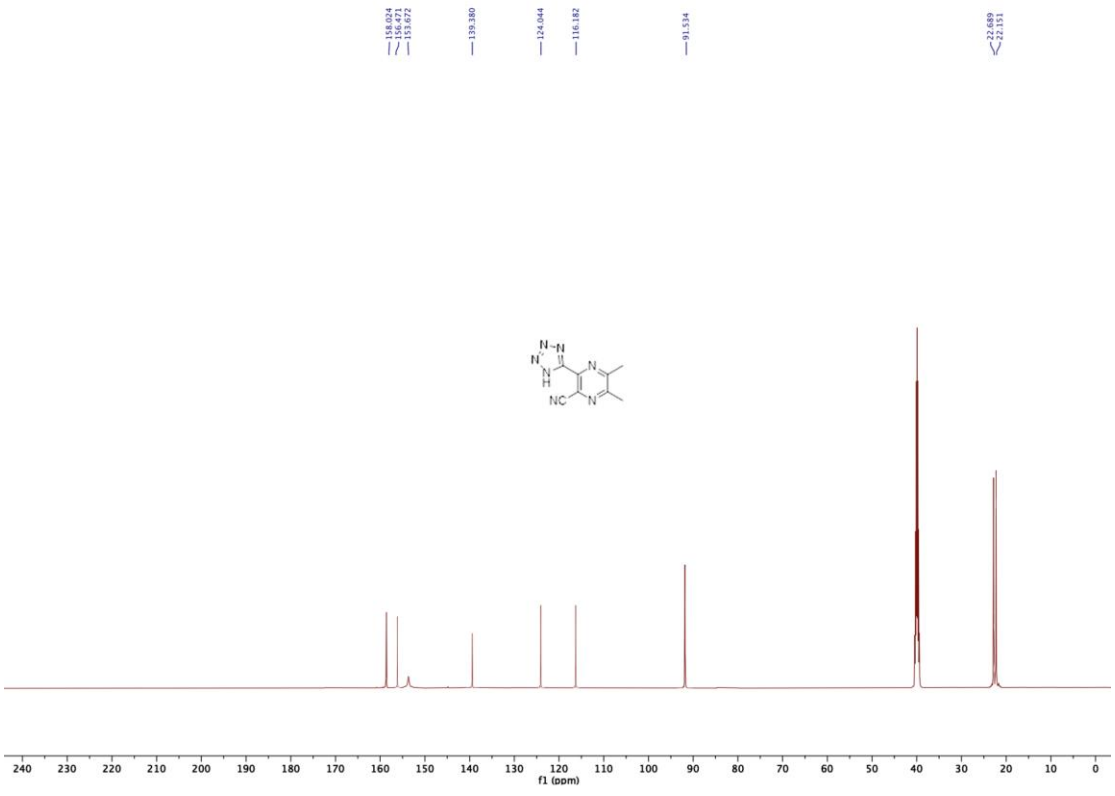
158.024
156.471
155.672
139.380
124.044
116.182
91.534
22.689
22.151
240 230 220 210 200 190 180 170 160 150 140 130 120 110 100 90 80 70 60 50 40 30 20 10 0
f1 (ppm)


7.56
7.54
7.54
7.53
7.53
7.52
7.51
7.51
7.49
7.48
7.47
7.46
7.41
7.40
7.40
7.39
7.38
7.37
7.37

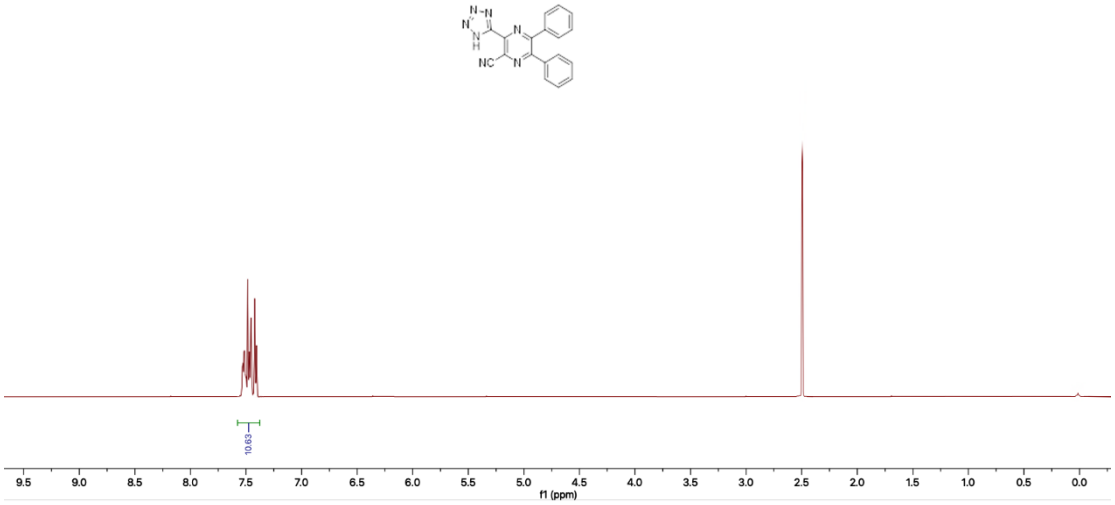
10.63
9.5
9.0
8.5
8.0
7.5
7.0
6.5
6.0
5.5
5.0
4.5
4.0
3.5
3.0
2.5
2.0
1.5
1.0
0.5
0.0
f1 (ppm)

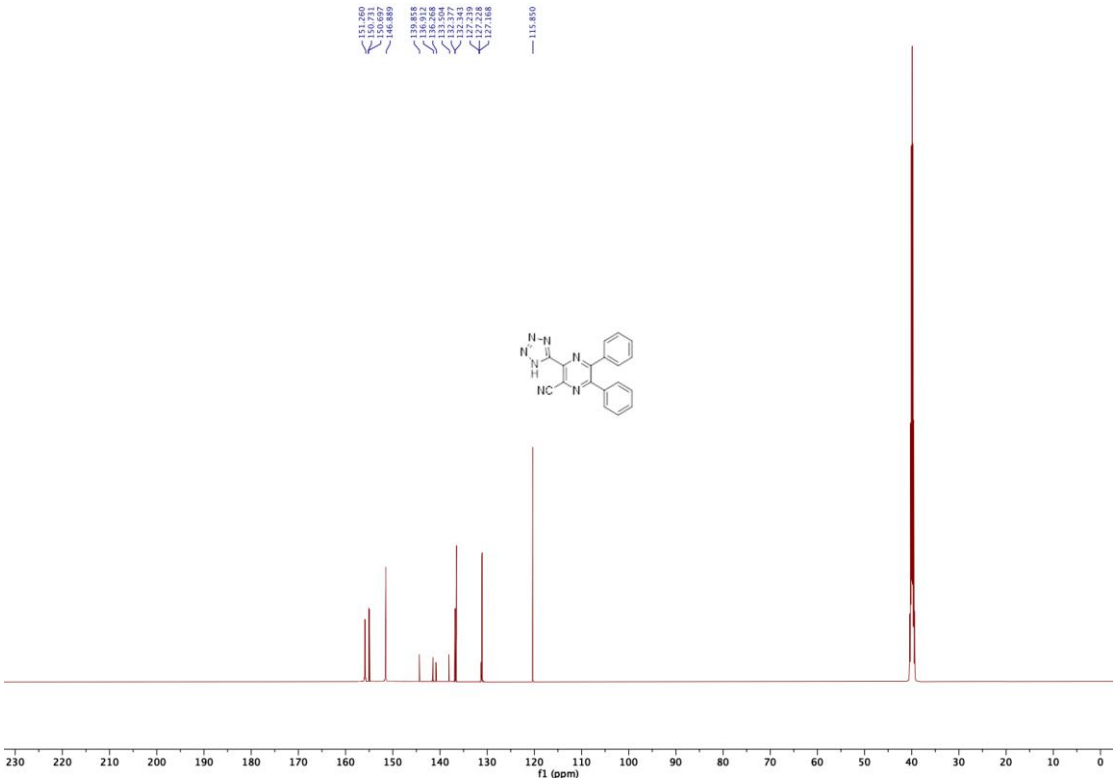
151.260
150.731
150.657
146.889
139.858
136.932
136.268
133.504
132.777
132.343
127.239
127.038
127.168
115.850
230
220
210
200
190
180
170
160
150
140
130
120
110
100
90
80
70
60
50
40
30
20
10
0
f1 (ppm)


7.67
7.67
7.66
7.66
7.65
7.65
7.55
7.55
7.54
7.53
7.53
7.32
7.31
7.30
7.29
7.28

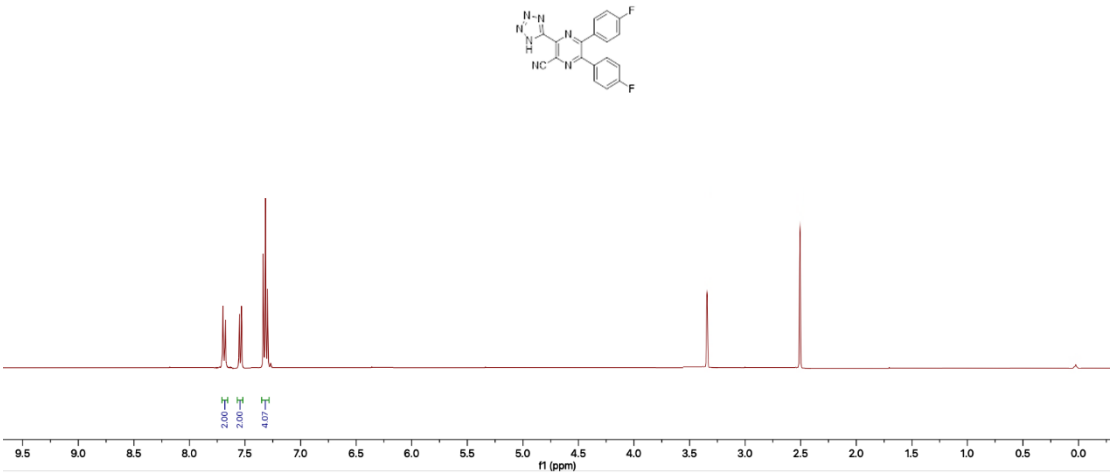
F
F
NC
2.00
2.00
4.07
9.5
9.0
8.5
8.0
7.5
7.0
6.5
6.0
5.5
5.0
4.5
4.0
3.5
3.0
2.5
2.0
1.5
1.0
0.5
0.0
f1 (ppm)

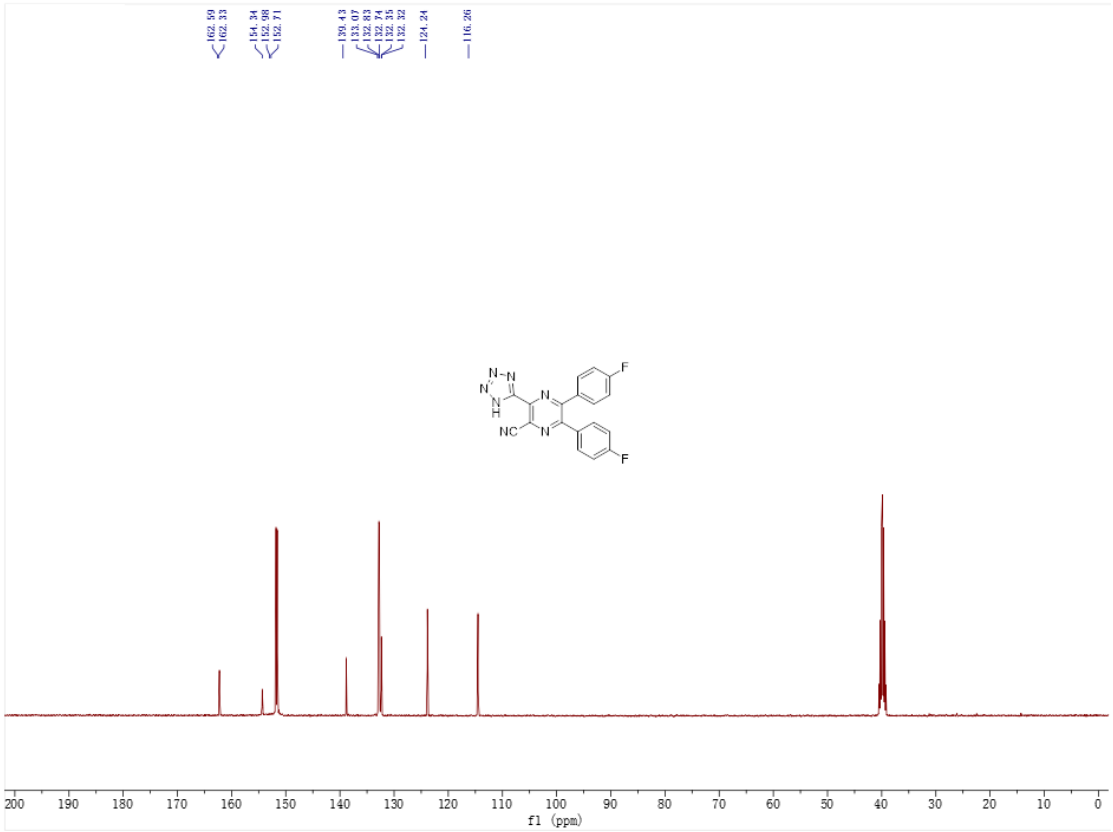
162.59
162.33
154.34
152.98
152.71
139.43
133.07
132.83
132.74
132.35
132.32
124.24
116.26
F
F
NC
200
190
180
170
160
150
140
130
120
110
100
90
80
70
60
50
40
30
20
10
0
f1 (ppm)

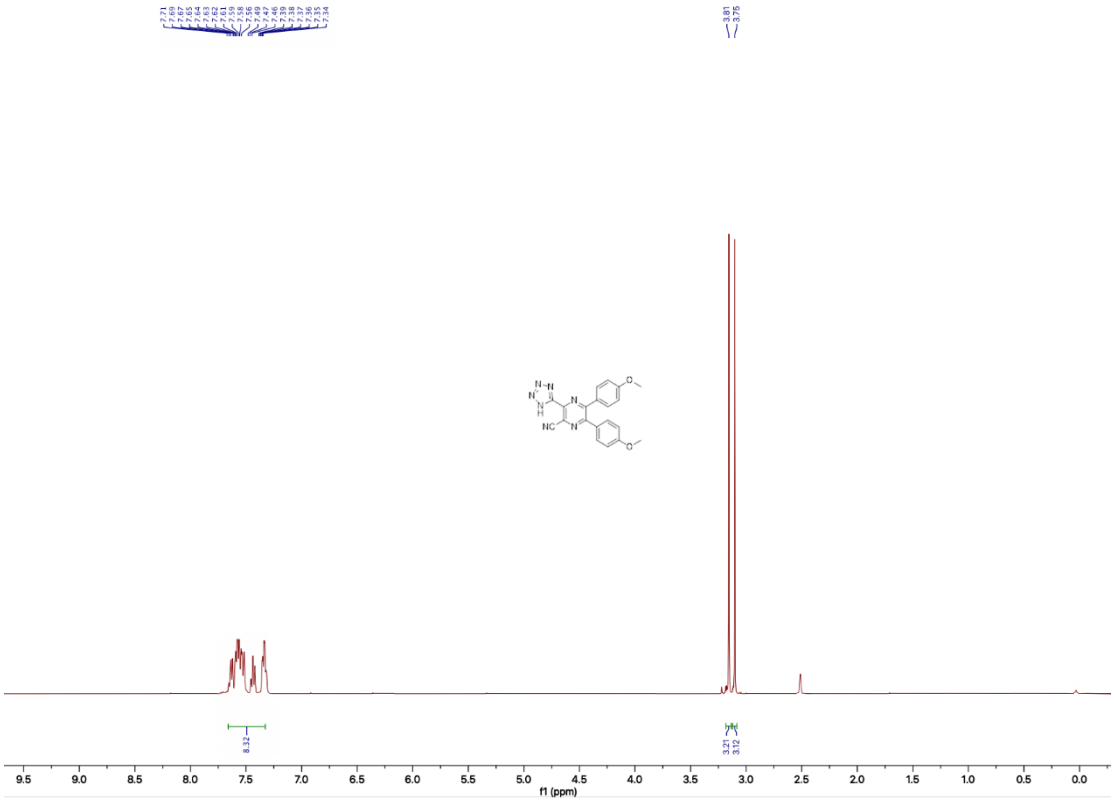
7.71
7.69
7.67
7.65
7.64
7.63
7.62
7.61
7.59
7.58
7.56
7.49
7.47
7.46
7.39
7.38
7.37
7.36
7.35
7.34
3.81
3.75
8.32
3.21
3.12
f1 (ppm)

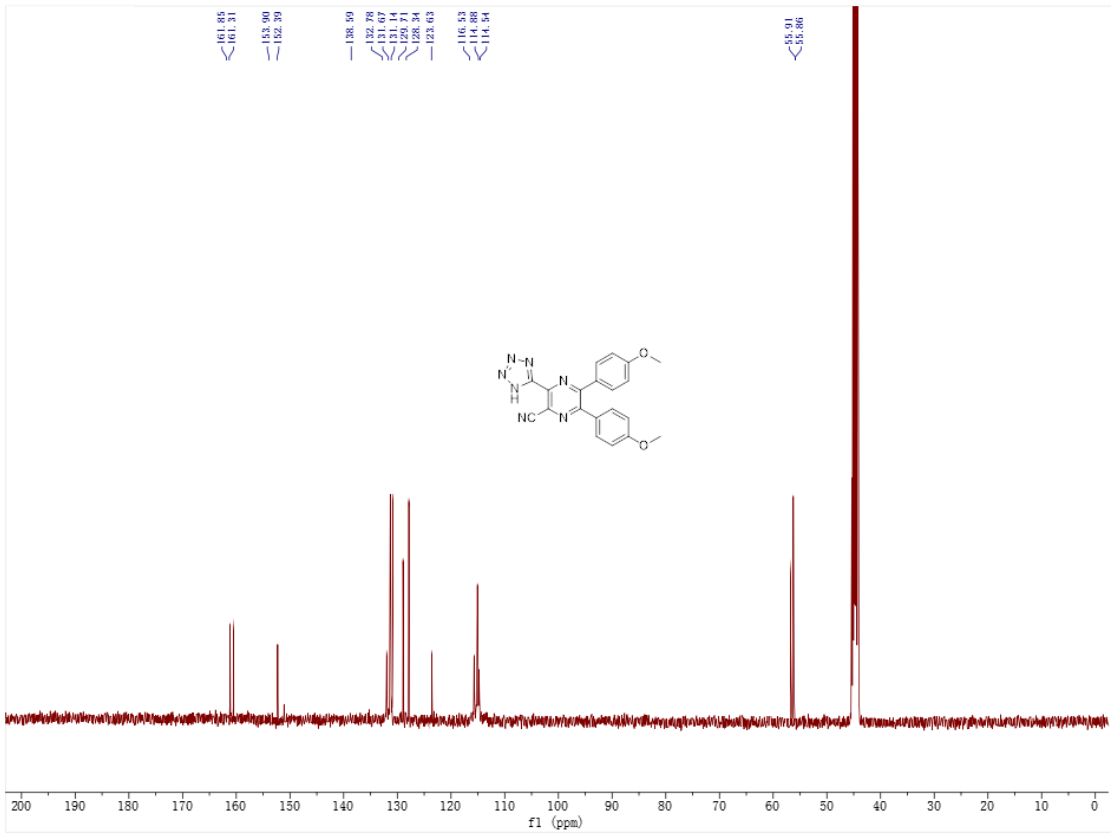
161.85
161.31
153.90
152.39
138.59
132.78
131.67
131.14
120.71
128.34
123.63
116.53
114.88
114.54
55.91
55.86
f1 (ppm)

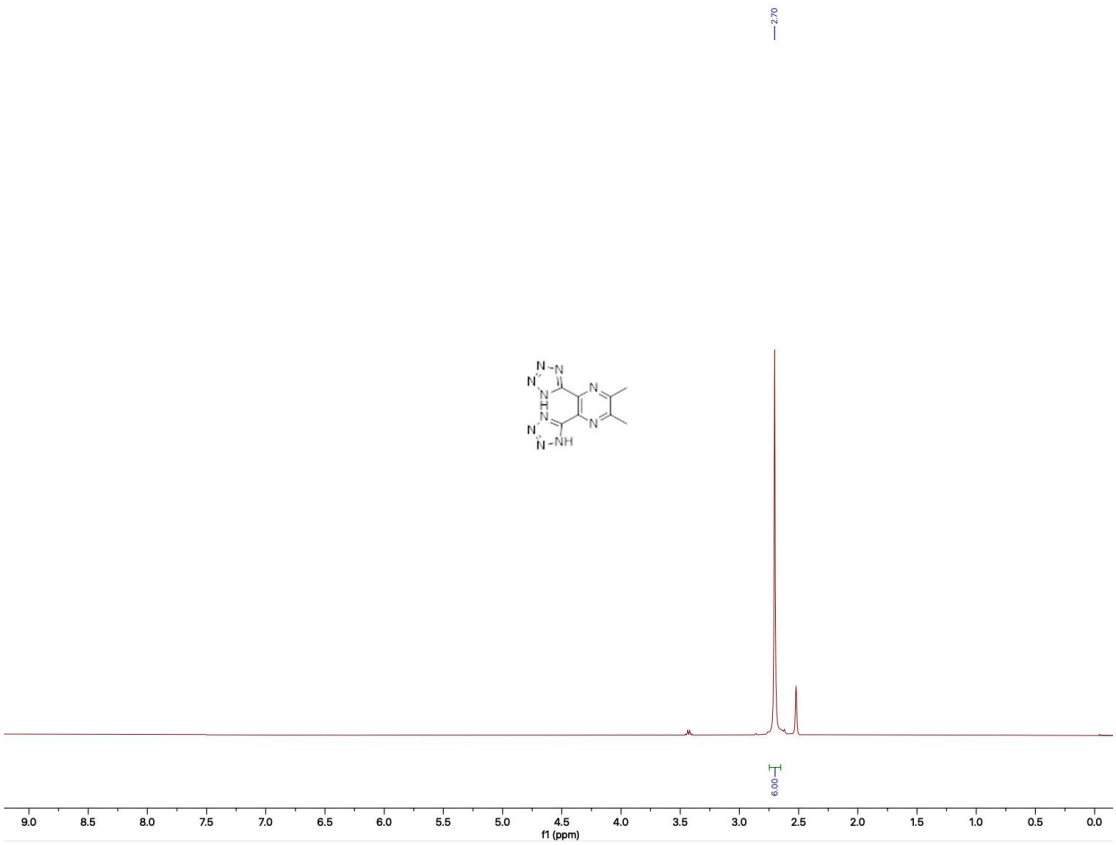
2.70
6.00
9.0 8.5 8.0 7.5 7.0 6.5 6.0 5.5 5.0 4.5 4.0 3.5 3.0 2.5 2.0 1.5 1.0 0.5 0.0
f1 (ppm)

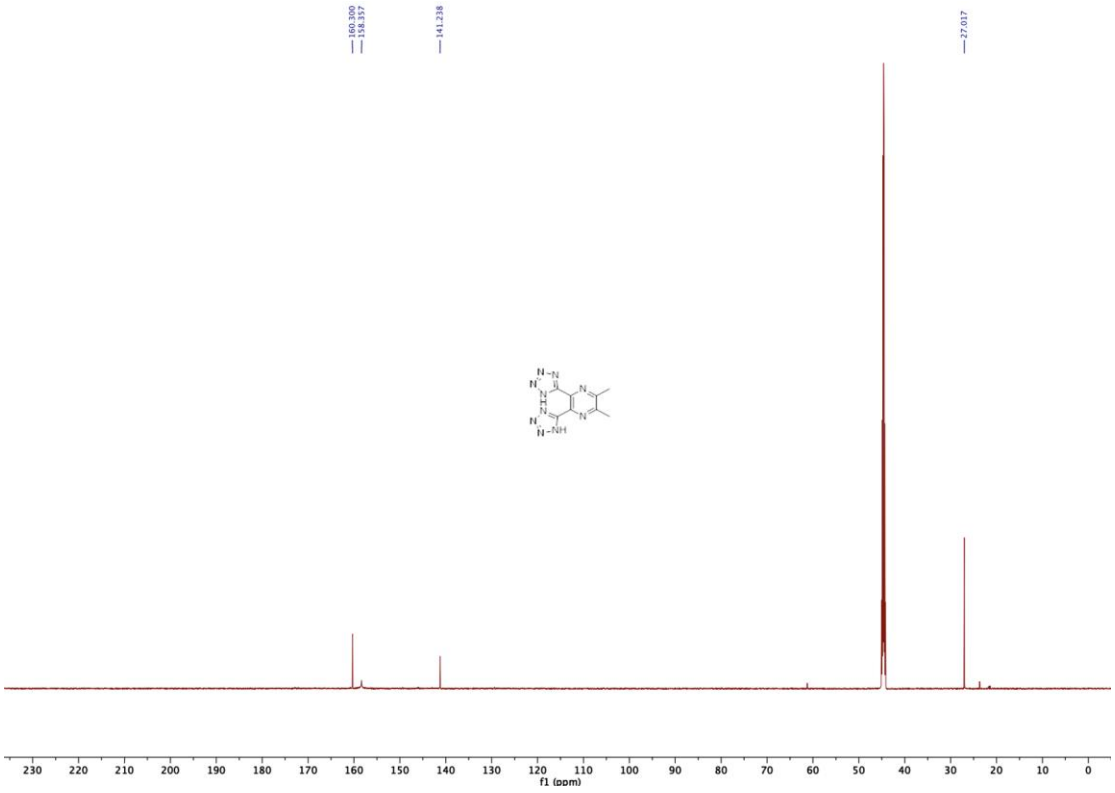
160.300
158.357
141.238
27.017
230 220 210 200 190 180 170 160 150 140 130 120 110 100 90 80 70 60 50 40 30 20 10 0
f1 (ppm)

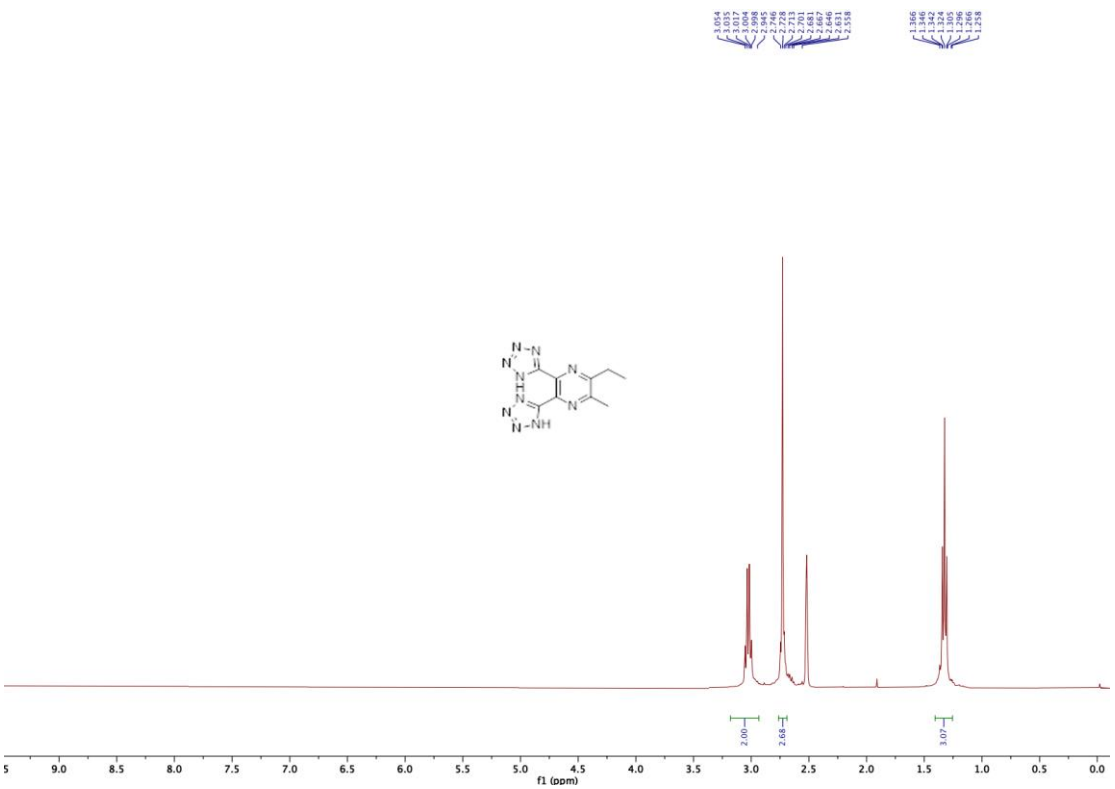
3.064
3.055
3.017
3.004
2.998
2.945
2.936
2.728
2.713
2.701
2.681
2.667
2.646
2.631
2.558
1.366
1.346
1.342
1.324
1.305
1.296
1.286
1.258
2.00
2.68
3.07
f1 (ppm)

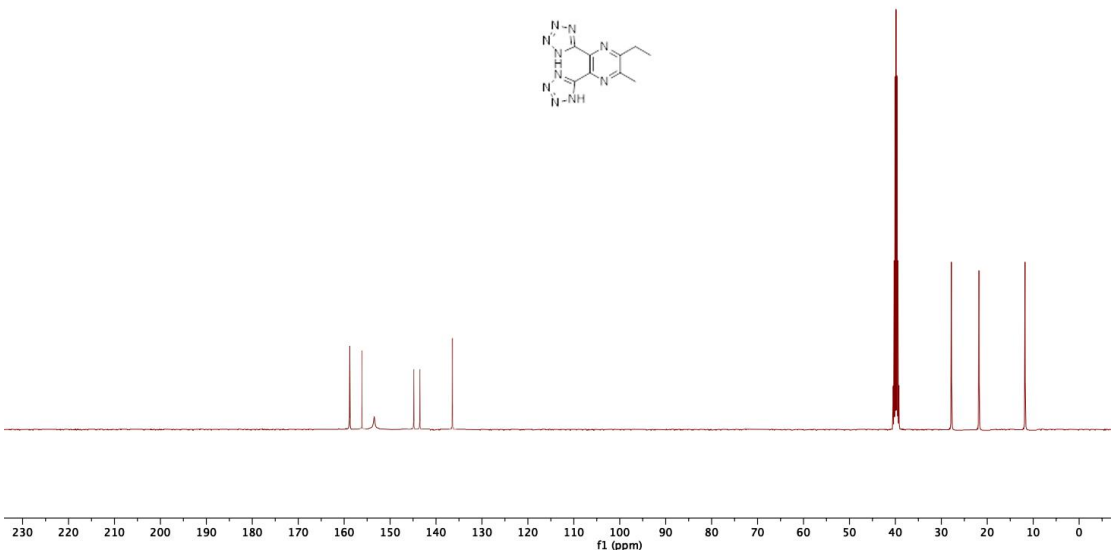
159.109
155.067
153.534
144.809
143.532
136.336
27.666
21.859
11.651
f1 (ppm)

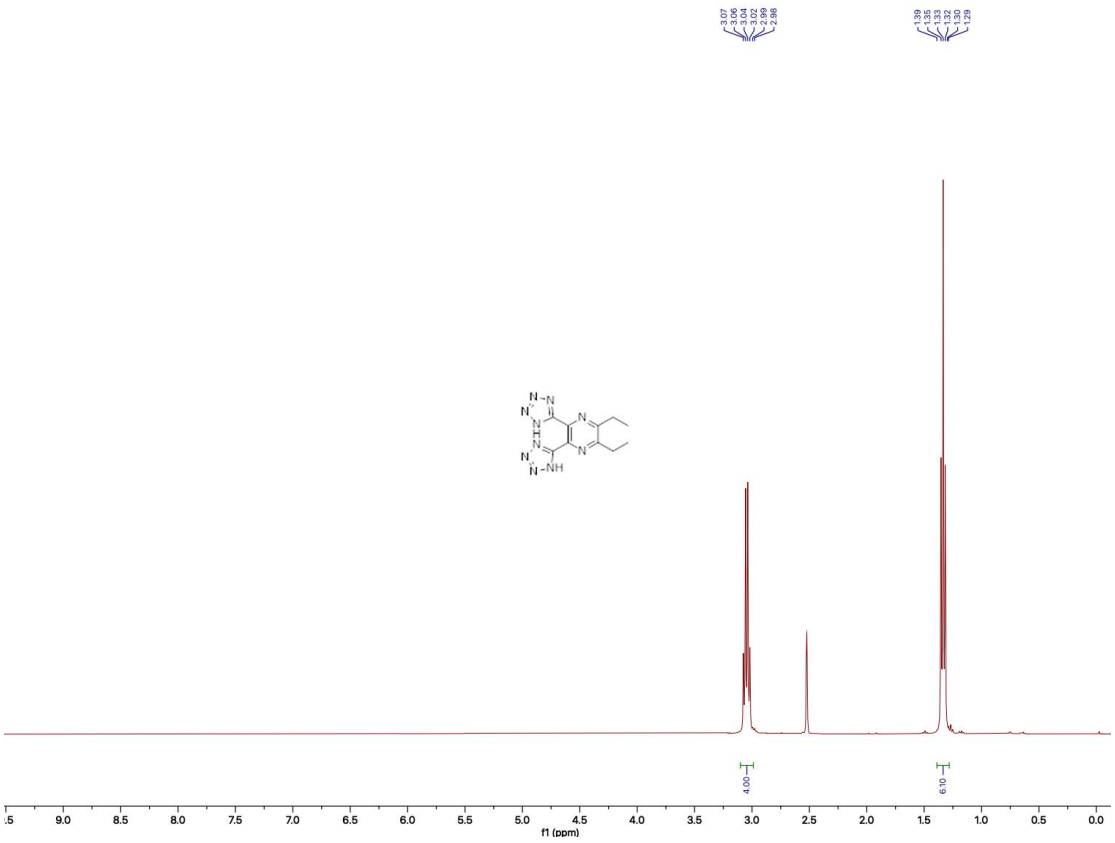
3.07
3.06
3.04
3.02
2.99
2.98
1.39
1.35
1.33
1.32
1.30
1.29
4.00
6.10
f1 (ppm)

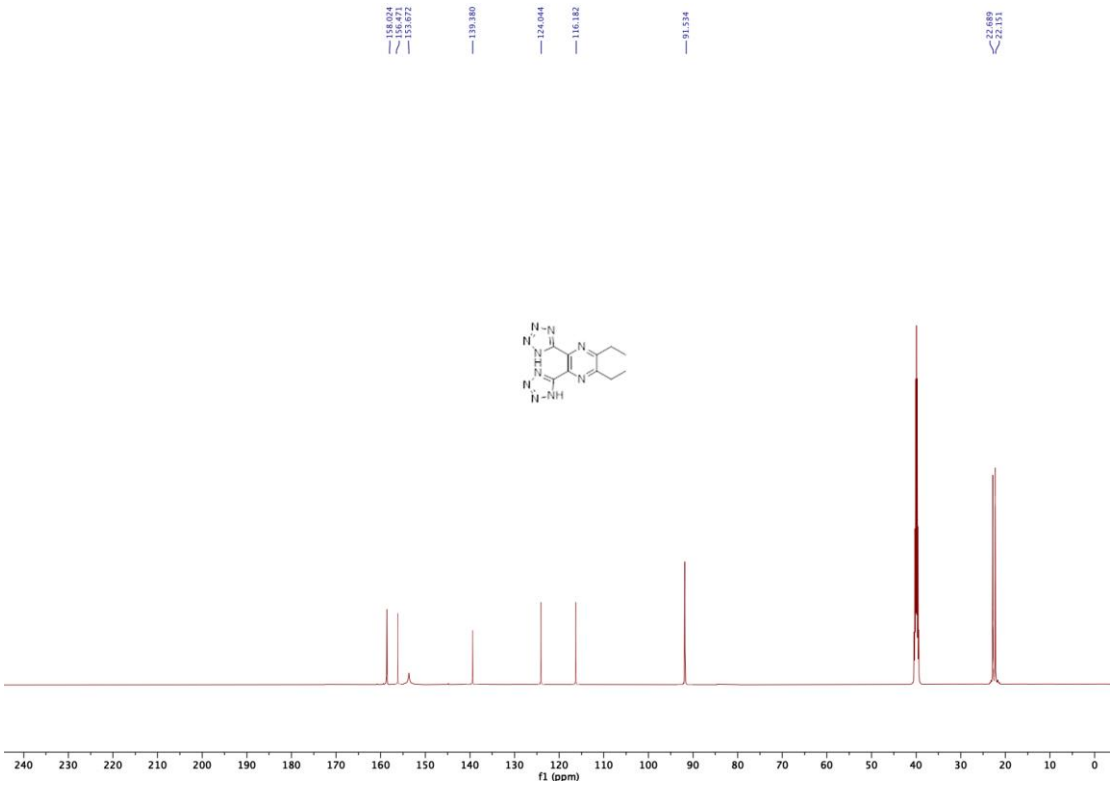
158.024
156.471
153.672
139.380
124.044
116.182
91.534
22.689
22.151
f1 (ppm)

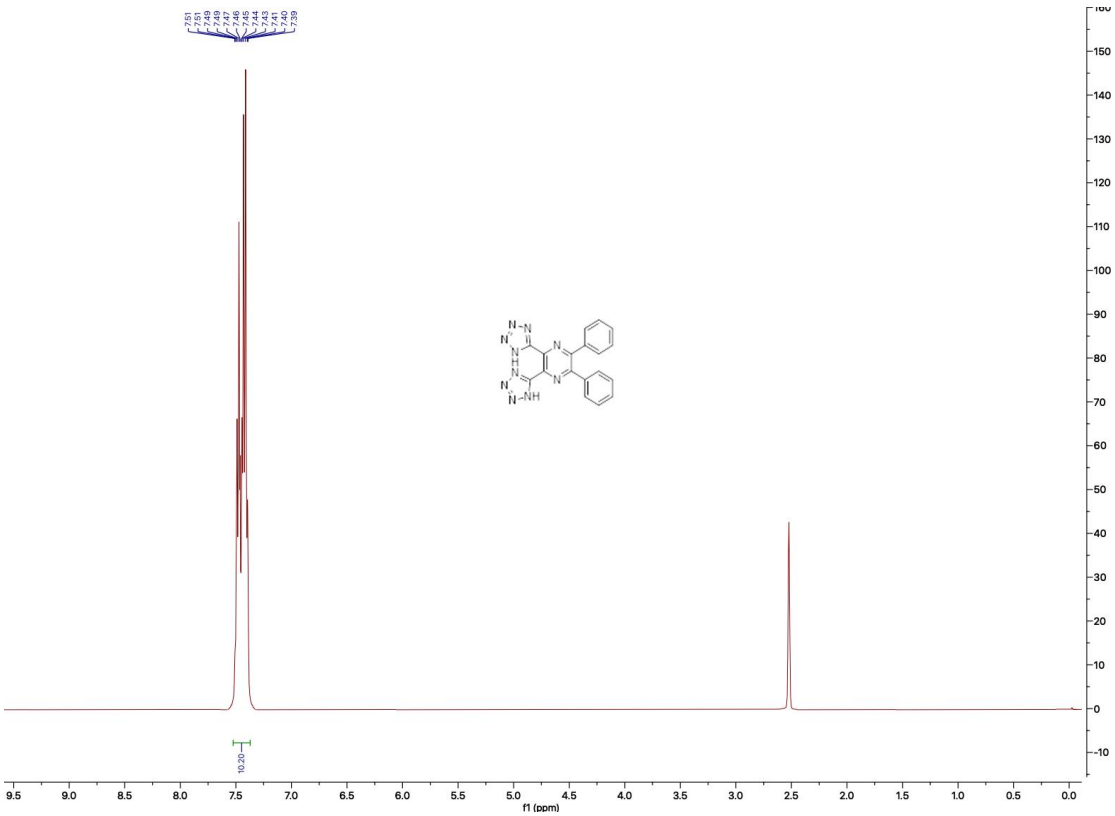
7.51
7.51
7.49
7.49
7.47
7.47
7.46
7.45
7.44
7.43
7.43
7.41
7.40
7.39
10.20
f1 (ppm)

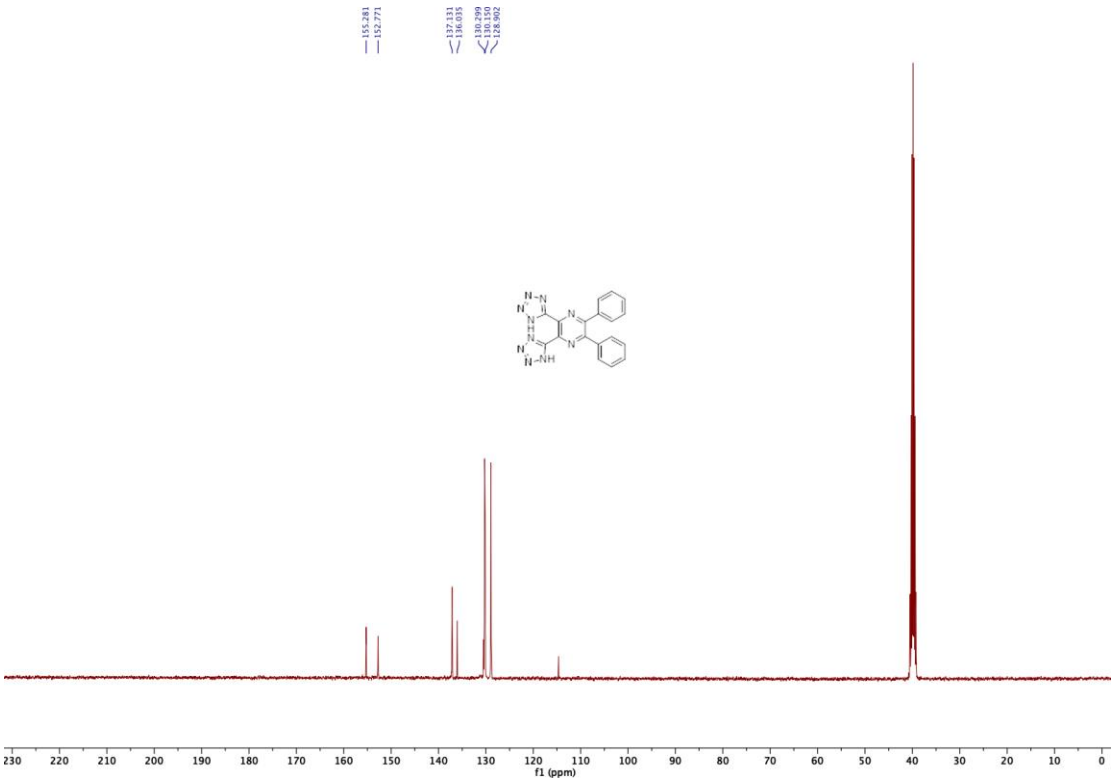
155.281
152.771
137.131
136.035
130.299
130.150
128.902
f1 (ppm)


7.70
7.68
7.67
7.66
7.66
7.59
7.56
7.55
7.54
7.53
7.53
7.52
7.31
7.30
7.29
7.29
7.28
7.26
7.25
7.24
7.23
7.22

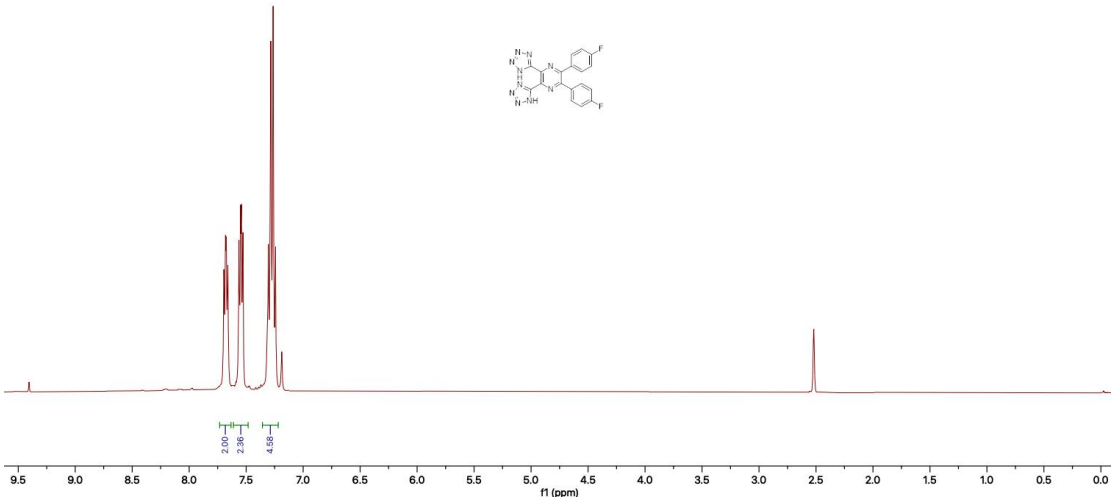
2.00
2.36
4.58
9.5
9.0
8.5
8.0
7.5
7.0
6.5
6.0
5.5
5.0
4.5
4.0
3.5
3.0
2.5
2.0
1.5
1.0
0.5
0.0
f1 (ppm)


164.63
164.33
162.98
162.58
154.33
153.70
151.86
132.76
132.70
116.39
116.24
116.09
115.95

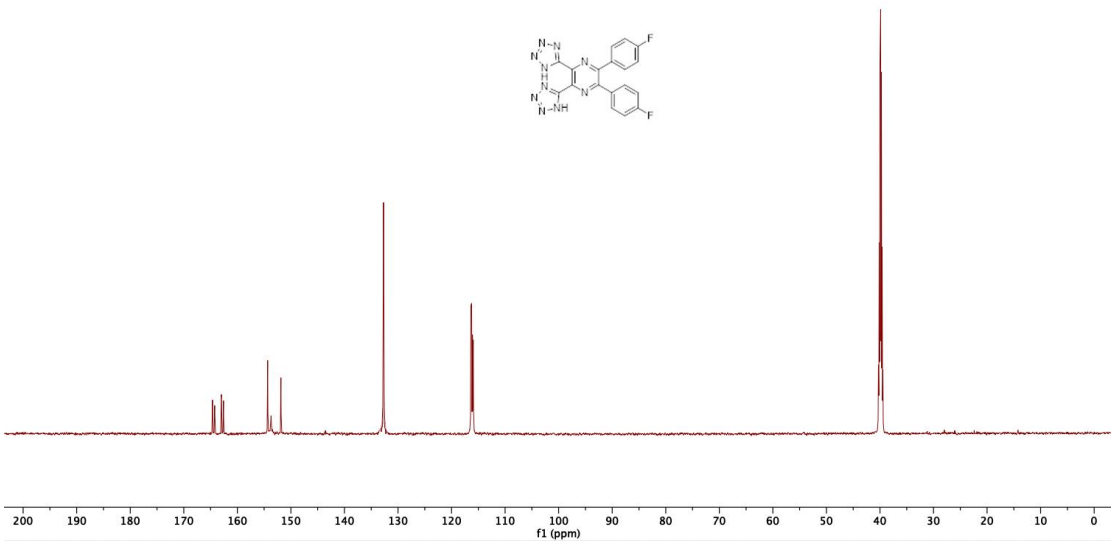
200
190
180
170
160
150
140
130
120
110
100
90
80
70
60
50
40
30
20
10
0
f1 (ppm)

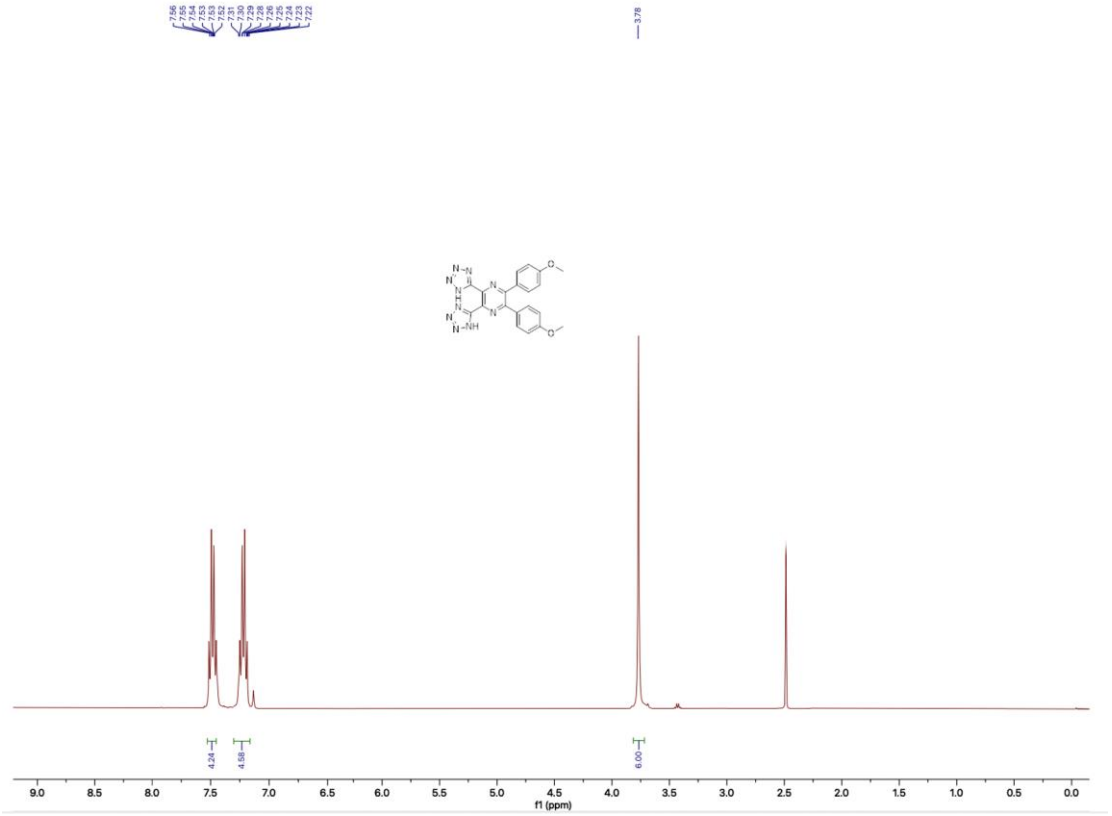
7.56
7.55
7.54
7.53
7.53
7.32
7.31
7.30
7.29
7.28
7.26
7.25
7.24
7.23
7.22
3.78
4.24
4.68
6.00
9.0
8.5
8.0
7.5
7.0
6.5
6.0
5.5
5.0
4.5
4.0
3.5
3.0
2.5
2.0
1.5
1.0
0.5
0.0
f1 (ppm)

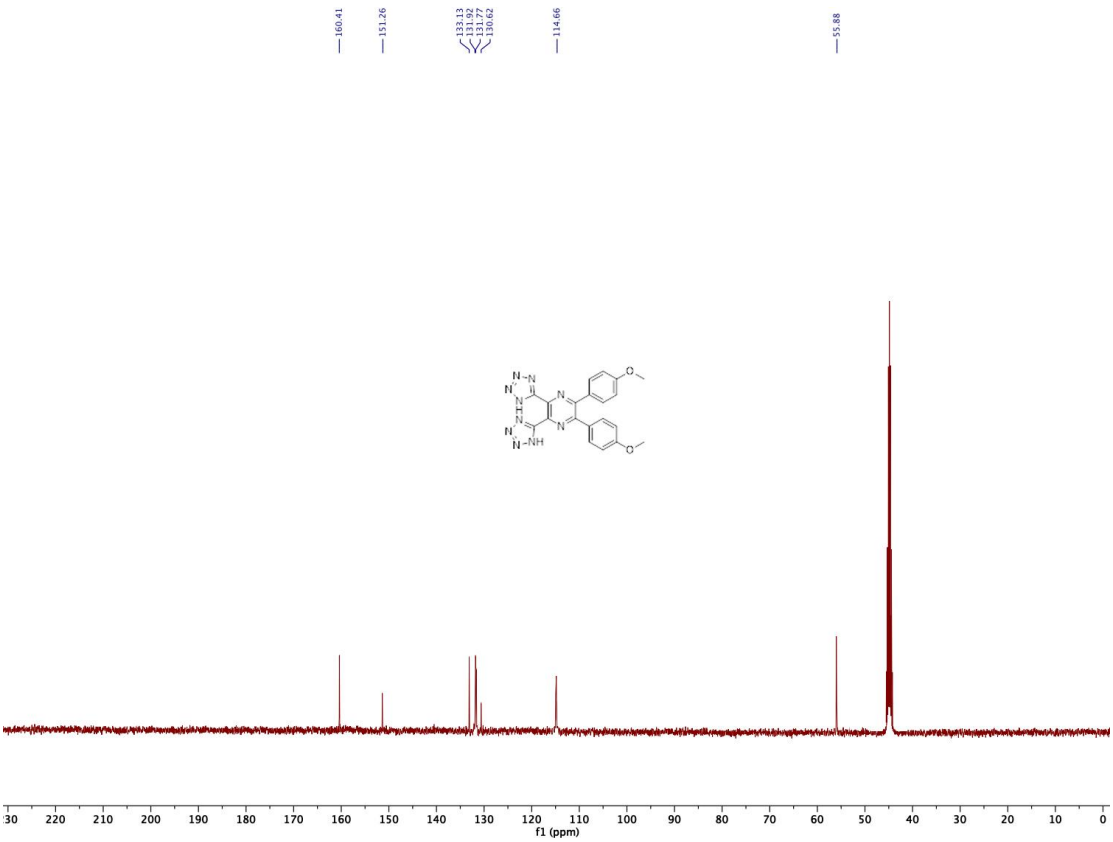
160.41
151.26
133.13
131.92
131.77
130.62
114.66
55.88
230
220
210
200
190
180
170
160
150
140
130
120
110
100
90
80
70
60
50
40
30
20
10
0
f1 (ppm)

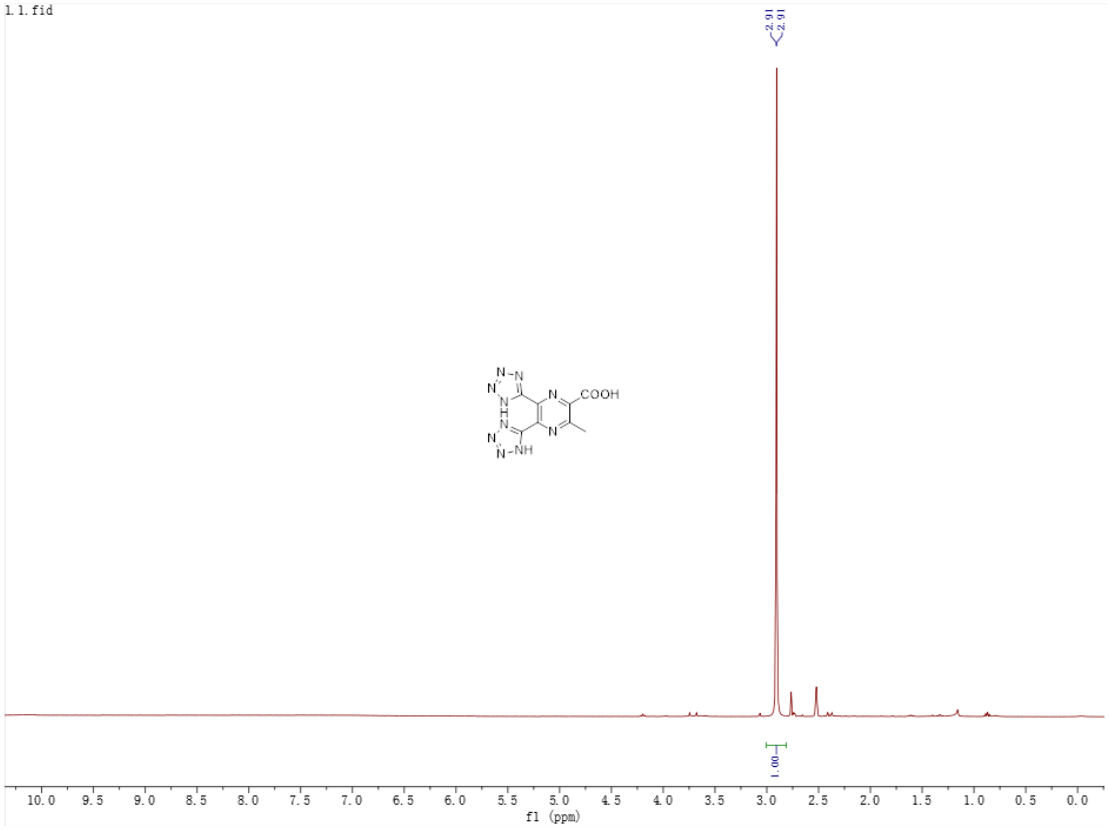
1_1.fid
2.91
2.91
COOH
NH
1.00
10.0 9.5 9.0 8.5 8.0 7.5 7.0 6.5 6.0 5.5 5.0 4.5 4.0 3.5 3.0 2.5 2.0 1.5 1.0 0.5 0.0
f1 (ppm)

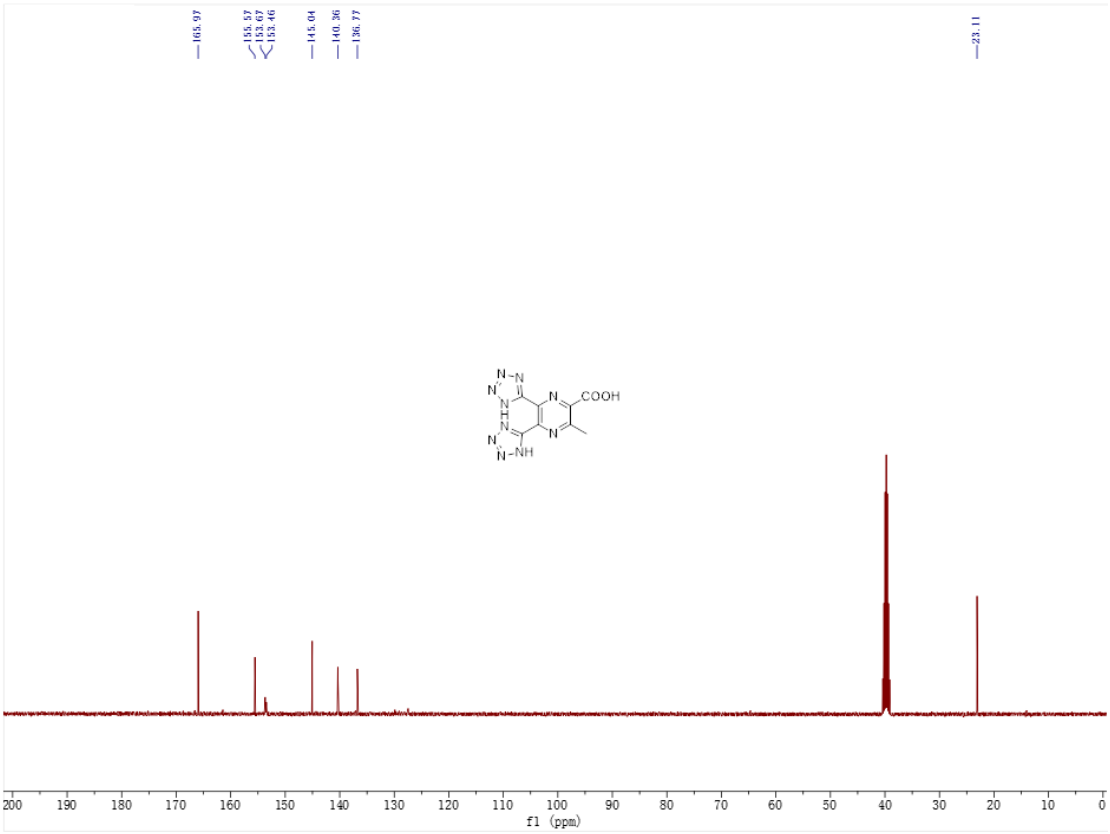
165.97
155.57
153.67
153.46
145.04
140.36
136.77
23.11
COOH
NH
200 190 180 170 160 150 140 130 120 110 100 90 80 70 60 50 40 30 20 10 0
f1 (ppm)